Numerical investigation of turbulent flow heat transfer and pressure drop of Al_2O_3/water nanofluid in helically coiled tubes

Ahmed Elsayed[1,2], Raya K. Al-dadah[1*], Saad Mahmoud[1] and Ahmed Rezk[2]

[1]School of Manufacturing and Mechanical Engineering, University of Birmingham, Birmingham, UK; [2]Faculty of Engineering, Mechanical Department, Alexandria University, Alexandria, Egypt

Abstract

Passive convective heat transfer enhancement can be achieved by improving the thermo-physical properties of the working fluid, changing flow geometry or both. This work presents a numerical study to investigate the combined effect of using helical coils and nanofluids on the heat transfer characteristics and pressure losses in turbulent flow regime. The developed computational fluid dynamics models were validated against published experimental data and empirical correlations. Results have shown that combining the effects of alumina (Al_2O_3) nanoparticles and tube coiling could enhance the heat transfer coefficient by up to 60% compared with that of pure water in straight tube at the same Reynolds number. Also, results showed that the pressure drop in helical coils using Al_2O_3 nanofluid for volume fraction of 3% was six times that of water in straight tubes (80% of the pressure drop increase is due to nanoparticles addition), while the effect of Reynolds number on the pressure drop penalty factor was found to be insignificant.

Keywords: nanofluids; helical coils; turbulent flow; heat transfer; CFD; fluent

*Corresponding author.
r.k.al-dadah@bham.ac.uk

Received 26 May 2013; revised 6 October 2013; accepted 8 January 2013

1 INTRODUCTION

Passive heat transfer enhancement techniques can improve compactness and thermal efficiency of heat exchangers. They are preferred due to their simplicity, longer operating life and lower cost and power requirements. Although there are various methods for achieving passive heat transfer enhancement, they all depend on changing flow geometry or improving the thermo-physical properties of the base working fluid. Helical coils have been shown to enhance single-phase heat transfer [1, 2], boiling heat transfer [3, 4] and condensation heat transfer [5, 6]. Nanofluids formed by mixing nanoparticles of metals or metal oxides such as copper, alumina, copper oxide with base fluid such as water, oil, ethylene glycol are investigated as a passive heat transfer enhancement technique. Nanoparticles improve the energy transport properties of the base fluid by increasing the effective thermal conductivity which enhances the heat transfer rate of the nanofluid. The applications using these nanofluids include engine cooling to reduce the engine weight and fuel consumption [7], increasing the critical heat flux in boilers [8] and developing compact heat exchangers for medical applications [9].

Recently, many researchers investigated numerically and experimentally the effect of nanofluids in enhancing the heat transfer in the turbulent flow regime in straight tubes. Li and Xuan [10] measured the heat transfer coefficient of Cu dispersed in water with 0.3–2% volume fraction in a straight tube 10 mm diameter and 0.8 m long. They developed a new correlation for Nusselt number in laminar and turbulent flow regimes as a function of volume concentration, Reynolds, Prandtl and Particle Peclet numbers. Nguyen *et al.* [11] investigated numerically the utilization of two nanofluids γ-Al_2O_3/water and γ-Al_2O_3/ethylene glycol (volume fractions 0–7.5%) for microprocessor cooling. The reduction in microprocessor temperature using the nanofluid was insignificant at lower levels of heat supplied. Rostamani *et al.* [12] numerically investigated turbulent flow of water with copper oxide (CuO), alumina (Al_2O_3) and titanium oxide (TiO_2) nanoparticles (volume concentrations 0–6%). Results showed that increasing the nanoparticles' volume concentration gave increased heat transfer coefficient and shear

International Journal of Low-Carbon Technologies 2015, 10, 275–282

doi:10.1093/ijlct/ctu003 Advance Access Publication 9 February 2014

stress. Also, the enhancement of heat transfer at lower Reynolds number was significant. Torii [13] measured convective heat transfer for water with nano-diamond particles (volume fractions 0.1, 0.4 and 1%) in 1-m long, 4-mm diameter straight tube. At volume fraction of 1% and for Reybolds numbers above 4000, significant enhancement was observed. Bianco *et al.* [14] numerically investigated turbulent flow in a straight tube 1 m long and 10 mm diameter. The enhancement ratio was predicted as 4, 19 and 33% for Al_2O_3 volume concentrations of 1, 4 and 6%, respectively. The computational fluid dynamics (CFD) prediction was close to the Pak and Cho correlation [15].

Work on combined passive enhancement techniques such as helical coils with nanofluids has been recently reviewed by Mangrulkar and Kriplani [16]. Regarding laminar flow, numerical simulation of Al_2O_3/water nanofluid flow in helical coils and curved tubes using the homogeneous approach [17, 18] and mixture models [19] was conducted for Reynolds number $<$2500 and volume fractions ranging from 1 to 4%. It is concluded that the mixture approach produces more accurate results but it is computationally intensive. On the other hand, the homogeneous approach was shown to be appropriate due to the negligible effect of particle diameter on the flow pattern [17–19]. CuO/water nanofluid with concentration $<$4% in helical coils was numerically modelled by [20–22] using the homogeneous approach investigating the effect of coil geometries (coil diameter ranging from 1800 to 1200 mm, tube diameter ranging from 32 to 52 mm) on pressure drop and heat transfer. They concluded that the Nusselt number increased by 68% while the pressure drop increased by 37% with decreasing the coil diameter. Also, the pressure drop and heat transfer behaviour of low-concentration CuO/water (0.1 and 0.2%) in helical coil were investigated experimentally and numerically by Akbaridoust *et al.* [23]. They have used both the homogeneous and dispersion models. Results have shown that the homogeneous model under-predicted the measured heat transfer enhancement while the modified dispersion model proved to better predict the experimental results.

Experimental work using various nanofluids and base fluids were reported in helical coils [24–30] at laminar flow. Mukeshkumar *et al.* [24] and Kahani *et al.* [25] experimentally tested Al_2O_3/water nanofluid with low volume concentration $<$1% and Reynolds numbers $<$4500 and 8600, respectively. Their results showed that heat transfer enhancement with respect to pure water flow in coils increased by up to 45% at 1% nanoparticles volume concentration. Hashemi and Akhavan-Behabadi [26] experimentally investigated the heat transfer and pressure drop characteristics of the pure oil and CuO/oil (concentration up to 2%) nanofluid flow inside a straight tube and a helical tube at low Reynolds number ($Re <$ 100). They reported a heat transfer enhancement of up to 18.7 and 30.4% was obtained for nanofluid flow with 2% wt. concentration compared with pure oil flow inside the straight tube and the helical tube, respectively. The Akhavan-Behabadi research group [27–29] experimentally investigated the heat transfer and pressure drop characteristics of the multi-walled carbon nanotubes (MWCNT)/oil nanofluids with weight concentration of 0.1, 0.2 and 0.4% in vertical helically coiled tubes. Their results indicated a heat transfer enhancement ratio of up to 10 times that of pure oil flow in straight tubes [27] while pressure drop of 3.5 times compared with base fluid in straight tube [29] were achieved.

Turbulent base fluid flow in helical coils was investigated by many researchers. Seban and Mclaughlin tested two coils using water with 7.37 mm internal diameter and coil to diameter ratio of 17 and 104 using direct electrical heating with constant heat flux. They correlated their experimental results with the thermophysical properties calculated at the film temperature (the average between bulk fluid temperature and wall temperature) [30]. Mori and Nakayama tested two coils with tube diameter to coil ratio of 18.7 and 40. They correlated their results with the thermo-physical properties calculated using the bulk average temperature [31].

Numerical and experimental research of heat transfer and pressure drop using nanofluids in helical coils in turbulent flow regime is very limited [16]. Kannadasan *et al.* [32] compared the water base fluid heat transfer in helical coil turbulent flow with CuO/water nanofluid at 0.1 and 0.2 volume fractions. At 0.2% volume fraction, 45 and 49% enhancement in Nusselt number were found for horizontal and vertical positions with an increase in pressure drop of 21 and 25%, respectively, compared with pure water flow in coils. Wallace [33] measured the heat transfer rate using nanofluids in a helically coiled cooler. However, the author did not report any measurements of heat transfer coefficients or wall temperatures. This work presents a CFD modelling study to investigate the heat transfer enhancement and pressure drop in turbulent flow with nanofluids through helical coil tubes. To model the heat transfer characteristics of nanofluids, researchers used different approaches including the homogeneous approach [12], the two-phase mixture approach [34], the Eulerian–Eulerian approach [35] and the Lagrangian trajectory model [36]. In the current investigation, the homogeneous approach is used as it requires less computational time and provides accurate prediction [12] and [35].

2 FLOW GOVERNING EQUATIONS AND THERMOPHYSICAL PROPERTIES

Al_2O_3 nanofluid was treated as incompressible, steady state, homogeneous and Newtonian fluid with negligible effect of viscous heating. The Navier–Stokes flow governing equations in the Cartesian co-ordinates are as follows:

Continuity:

$$\frac{\partial}{\partial x_i}(\rho u_i) = 0. \tag{1}$$

Momentum:

$$\frac{\partial}{\partial x_j}(\rho u_i u_j) = -\frac{\partial P}{\partial x_i} + \rho g_i + \frac{\partial}{\partial x_j}\left[\mu\left(\frac{\partial u_i}{\partial x_j} + \frac{\partial u_j}{\partial x_i}\right)\right] + \frac{\partial}{\partial x_j}(-\rho\overline{u'_i u'_j}). \quad (2)$$

Energy:

$$\frac{\partial}{\partial x_i}(\rho u_i T) = \frac{\partial}{\partial x_j}\left((\Gamma + \Gamma_t)\frac{\partial T}{\partial x_j}\right)\Gamma = \frac{\mu}{Pr} \quad \text{and} \quad \Gamma_t = \frac{\mu_t}{Pr_t}. \quad (3)$$

Γ and Γ_t are the molecular thermal diffusivity and turbulent thermal diffusivity, respectively. The Boussinesq hypothesis is used to relate the Reynolds stresses (last term in momentum equation) to the mean velocity as:

$$(-\rho\overline{u'_i u'_j}) = \mu_t\left(\frac{\partial u_i}{\partial x_j} + \frac{\partial u_j}{\partial u_i}\right). \quad (4)$$

The turbulent viscosity term is computed using the k-ε turbulent model with two additional equations namely turbulent kinetic energy(TKE, k) and turbulent dissipation rate (ε) so that:

$$\mu_t = \rho C_\mu \frac{k^2}{\varepsilon}. \quad (5)$$

The modelled equation of the TKE, k, is:

$$\frac{\partial}{\partial x_i}(\rho k u_i) = \frac{\partial}{\partial x_j}\left[\left(\mu + \frac{\mu_t}{\sigma_k}\right)\frac{\partial k}{\partial x_j}\right] + G_k + \rho\varepsilon, \quad (6)$$

where $\rho\varepsilon$ is the turbulence destruction rate (TDR) of TKE and GK is the rate of generation of the TKE given by:

$$G_k = -\rho\overline{u'_i u'_j}\frac{\partial u_j}{\partial x_i}. \quad (7)$$

The dissipation rate of the TDR, ε, is given by the following equation:

$$\frac{\partial}{\partial x_i}(\rho\varepsilon u_i) = \frac{\partial}{\partial x_j}\left[\left(\mu + \frac{\mu_t}{\sigma_\varepsilon}\right)\frac{\partial \varepsilon}{\partial x_j}\right] + C_{1\varepsilon}\frac{\varepsilon}{k}G_k + C_{2\varepsilon}\rho\frac{\varepsilon^2}{k}. \quad (8)$$

The boundary values for the turbulent quantities near the wall were determined using the two layers enhanced wall treatment. The values of the empirical constants in the turbulence transport equations are as follow:

$$C_\mu = 0.09, \quad C_{1\varepsilon} = 1.44, \quad C_{2\varepsilon} = 1.92, \quad \sigma_k = 1, \quad \sigma_\varepsilon = 1.3 \quad \text{and} \quad Pr_t = 0.85.$$

Pr_t is the turbulent Prandtl number at the wall. These default values have been determined from experiments with air and water for fundamental turbulent shear flows. They have been found to work fairly well for a wide range of wall-bounded and free shear flows [37]. The effective thermo-physical properties of the nanofluid are [38]:

Density:

$$\rho_{nf} = (1-\varphi)\rho_{bf} + \rho_p\varphi. \quad (9)$$

Specific heat:

$$C_{nf} = ((\rho C)_p\varphi + (\rho C)_{bf}(1-\varphi))/\rho_{nf}. \quad (10)$$

Thermal conductivity:

$$\lambda_{nf} = (1 + 4.5503\varphi)\lambda_{bf}. \quad (11)$$

Dynamic viscosity:

$$\mu_{nf} = \exp(4.91\varphi/(0.2092 - \varphi))\mu_{bf}, \quad (12)$$

where *nf*, *bf* and *P* denote the nanofluid, base fluid and particle, respectively. The base fluid thermo-physical properties have been fitted as polynomial functions in temperature (Kelvin) using Engineering Equation Solver EES data as shown in equations (13–15).

$$\rho_{bf} = 2813.77E(-01) + 6351.93E(-03)T - 1761.03E(-05)T^2 + 1460.96E(-08)T^3, \quad (13)$$

$$k_{bf} = -1056.42E(-03) + 1011.33E(-05)T - 1772.74E(-08)T^2 + 7994.88E(-12)T^3, \quad (14)$$

$$\mu_{bf} = 9684.22E(-05) - 821.53E(-06)T + 2345.21E(-09)T^2 - 2244.12E(-12)T^3. \quad (15)$$

These properties were formulated as user-defined functions (UDF) subroutines and incorporated into Fluent 6.3 solver. Fluent is a computational fluid dynamic software based on finite volume method for solving the continuity, momentum and energy partial differential equations of fluid flow.

3 MODELLING DESCRIPTIONS AND VALIDATION

3.1 Straight tube

The CFD analysis for the base fluid flow in straight tube was investigated to provide a reference case using the experimental setup of Williams *et al.* [38]. Half of the 9.4-mm internal diameter and 2819-mm long tube has been modelled using the symmetry along the tube axis to reduce the computational time. Two adiabatic sections with 1 and 0.5 m long, respectively, were positioned before and after the heated section to ensure fully developed flow. The boundary conditions at the inlet and outlet of the tube was specified as velocity inlet and pressure outlet, respectively. The heated section was meshed with 40 and 1600 nodes in the radial and axial directions, respectively. The 1 and 0.5 m adiabatic sections were meshed with 40 × 800 and 40 × 400 nodes in the radial and axial directions. The second-order upwind scheme was utilized for discretizing the energy and momentum equations, turbulence kinetic energy and turbulence dissipation rate. Uniform heat flux was applied to the heated

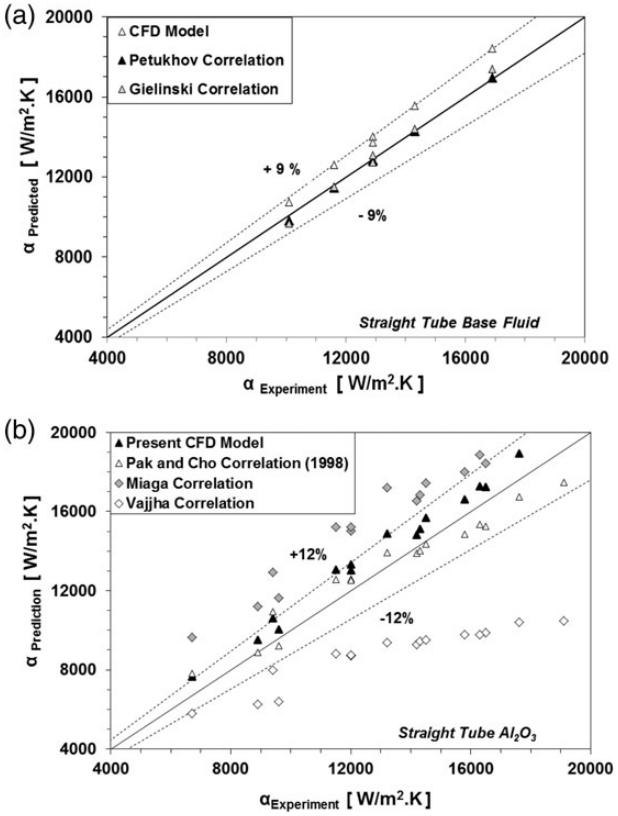

Figure 1. *Validation of straight tube for (**a**) base fluid and (**b**) nanofluid in straight tubes.*

section. The coupled algorithm was used with Courant number set to one for solving the pressure–velocity coupling [39]. Courant number is the ratio of the time step to the cell residence time which expresses the ratio of the distance travelled by a disturbance in one time step to the length of a computational distance step. In the CFD calculations, the Courant number must be less than or equal to unity so as to ensure the convergence of the discretized equations.

The average heat transfer coefficient was calculated using the average heated wall temperature and average fluid temperature at the inlet and outlet of the heated section. Figure 1a shows the CFD predicted heat transfer coefficient and those reported by Williams *et al.* [38] at various Reynolds numbers with $\pm 9\%$ agreement with experimental data and those predicted by Petukhov (Equation (16)) and Gnielinski correlations (Equation (17)) who correlated the Nusselt number as a function of Reynolds and Prandtl numbers in the following form [40].

Petukhov correlation:

$$Nu = \frac{(f/8)Re\,Pr}{1.07 + 12.7(f/8)^{0.5}(Pr^{(2/3)} - 1)}. \tag{16}$$

Gnielinski correlation:

$$Nu = \frac{(f/8)(Re - 1000)Pr}{1 + 12.7(f/8)^{0.5}(Pr^{(2/3)} - 1)}, \tag{17}$$

where $f = (1.82\log_{10}(Re) - 1.64)^{-2}$

Figure 1b presents the predicted heat transfer coefficient of Al_2O_3 nanofluid in a straight tube compared with the experimental results of Williams *et al.* [38] at volume concentration ratios of 0.9, 1.8 and 3.6% at Reynolds numbers ranging from 8000 to 60 000 with $\pm 12\%$ agreement. The Pak and Cho correlation (Equation 18, [15]) was in a good agreement with the CFD prediction. On the other hand, the Vajjha *et al.* (Equation 19, [41]) correlation tends to under predict the experimental measurement and the Maiga correlation (Equation 20, [42]) was found to over predict the experimental results.

Pak and Cho correlation [15]:

$$Nu_{nf} = 0.021Re_{nf}^{0.8}Pr_{nf}^{0.5}. \tag{18}$$

Vajjha correlation [41]:

$$Nu_{nf} = 0.065(Re_{nf}^{0.65} - 60.22)(1 + 0.0169\varphi^{0.15})Pr_{nf}^{0.542}. \tag{19}$$

Maiga correlation [42]:

$$Nu_{nf} = 0.085Re_{nf}^{0.71}Pr_{nf}^{0.35}. \tag{20}$$

3.2 Helically coiled tube

For simulating the flow of a base fluid inside helically coiled tube, coil with tube length and diameter similar to those used in the straight tube analysis was used. The coil pitch was selected as 15 mm and number of turns of 5 leading to a coil diameter of 179.5 mm. The discritization schemes utilized were second order for energy, first order for momentum and SIMPLEC algorithm with skewness factor of one for coupling the velocity and pressure parameters. The mesh contains 1 026 000 cells with the number of nodes in the axial direction are 500, 1500 and 250 for the inlet straight, helically coiled, outlet straight tubes, respectively. Tri-quad elements has been utilized to mesh the inlet face and hex/wedge cooper elements used to mesh the coil volume with six layers close to the wall and 50 nodes in the radial direction as shown in Figure 2. The mesh quality has been checked by controlling the turbulent wall function y^+ value to be <5 as depicted in Figure 3. The required simulation time for each run was 8 h using 2.4 GHz core Quad processor with 2 GB RAM memory computer.

Figure 4 compares the CFD predicted heat transfer coefficients with the empirical correlations (Equations 21–22) of Seban and Mclaughlin [30] and Mori and Nakayam [31] at a heat flux of 30 kW/m^2. The percentage mean absolute derivation between the CFD prediction and those of the Seban

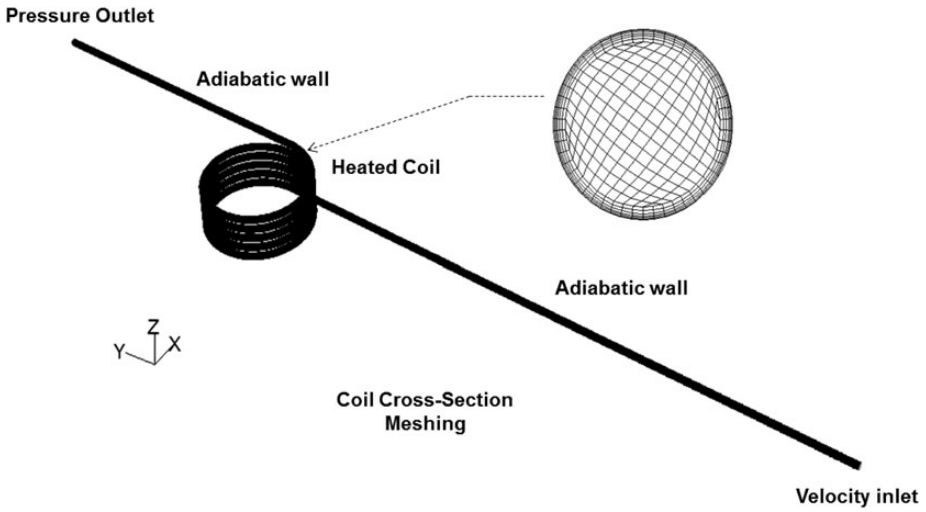

Figure 2. *3D mesh of helical coil using tri-quad mesh.*

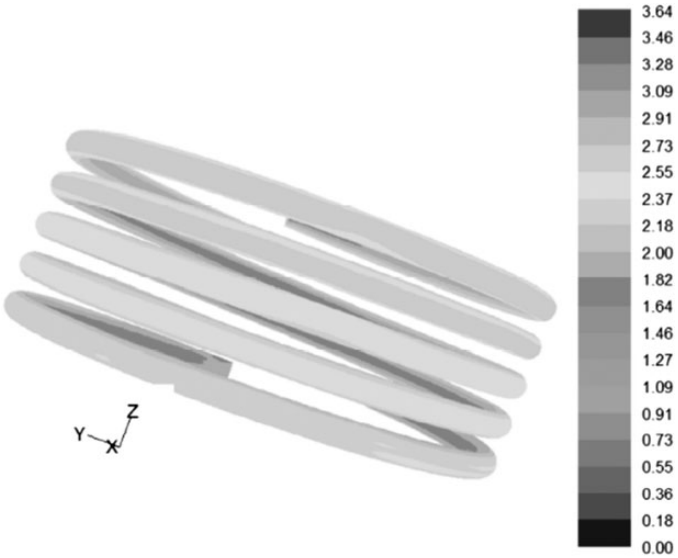

Figure 3. *Turbulence Wall function* y+.

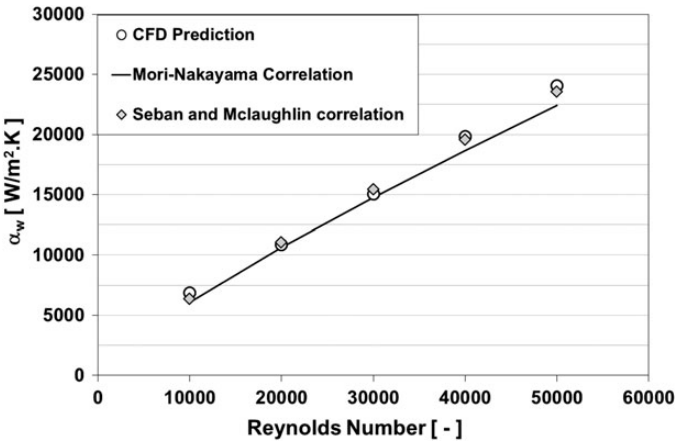

Figure 4. *CFD prediction and empirical correlation for water flow in coils.*

and Mclaughlin [30] correlation was found to be less than $\pm 3.2\%$.

$$\alpha_{\text{Seban-Mclaughlin}} = 0.023 Re^{0.85} Pr^{0.4} \left(\frac{d_i}{d_{\text{coil}}}\right)^{0.1} \frac{\lambda}{d_i}. \qquad (21)$$
$$6000 \leq Re \leq 65\,600 \quad 2.9 < Pr < 5.7.$$

$$\alpha_{\text{Mori-Nakayama}} = \frac{1}{41} Re^{5/6} Pr^{0.4} \left(\frac{d_i}{d_{\text{coil}}}\right)^{(1/12)} \left(1 + 0.061/(Re(d_i/d_{\text{coli}})^{2.5})^{(1/6)}\right) \frac{\lambda}{d_i}. \qquad (22)$$
$$10\,000 \leq Re \leq 200\,000 \qquad Pr > 1.$$

4 HEAT TRANSFER AND PRESSURE DROP OF NANOFLUIDS IN HELICAL COILS

This section investigates the effect of using nanofluids on the heat transfer and pressure drop for helical coils. Similar methodology for modelling the nanofluid flow in straight tubes (Section 3.1) was used. Figure 5 compares the velocity contours of the nanofluid (concentration 2%, Figure 5a) with that of the base fluid (Figure 5b) at Reynolds number of 20 000 and different positions (inlet, 1 turn, 2.5 turns and 5 turns) in the coil. This figure shows that, for the same Reynolds number, higher velocities were produced due to the larger kinematic viscosity of the nanofluid. The flow enters the coil as hydrodynamically fully developed turbulent flow as shown by the coil inlets in Figure 5a and b. Inside the helical coil, the fluid elements with high velocities are pushed to the outer side of the coil due to the centripetal force thus generating secondary flow in the coil that results in better mixing of bulk fluid and decreases the wall temperature.

Figure 6 shows the variation of the heat transfer enhancement ratio (nanofluid in the helical coil divided by that of base fluid in the straight tube) with the volume concentrations of the

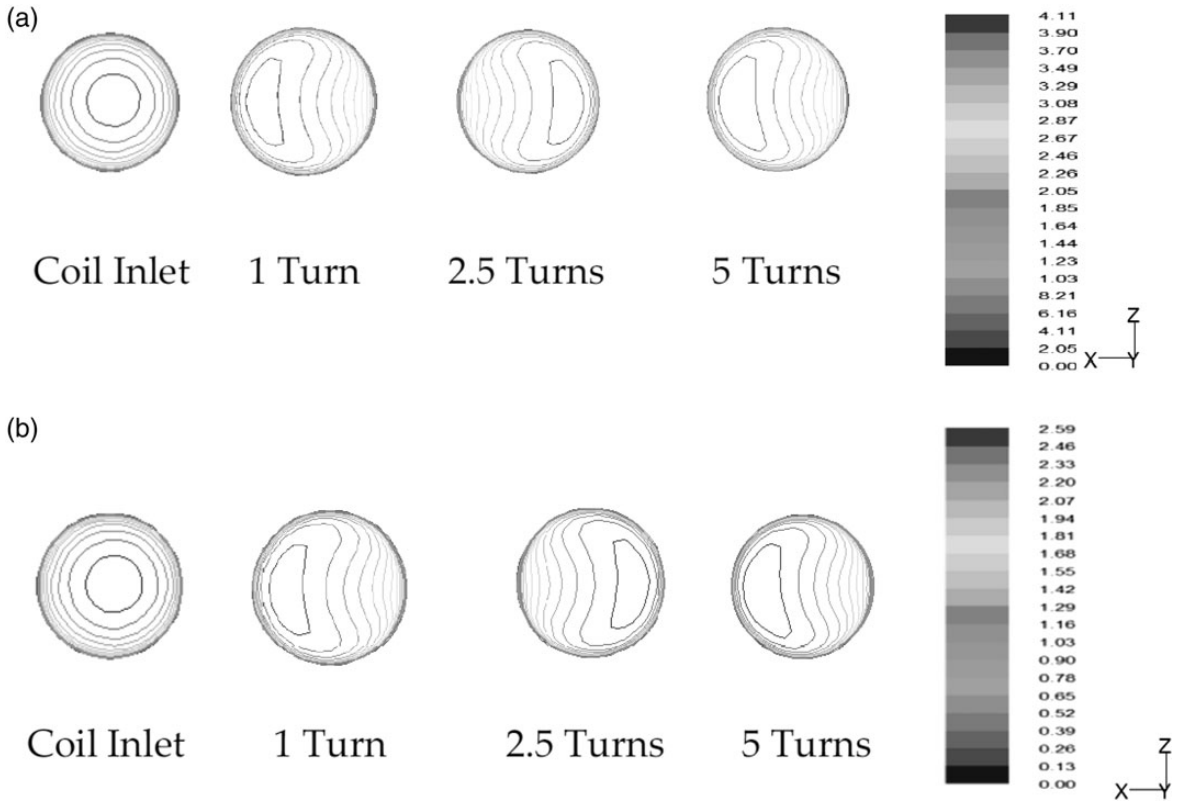

Figure 5. *Velocity contours cross section parallel to coil inlet* (y = *0) at* Re = *20 000: (**a**) nanofluid concentration 2%; (**b**) pure water.*

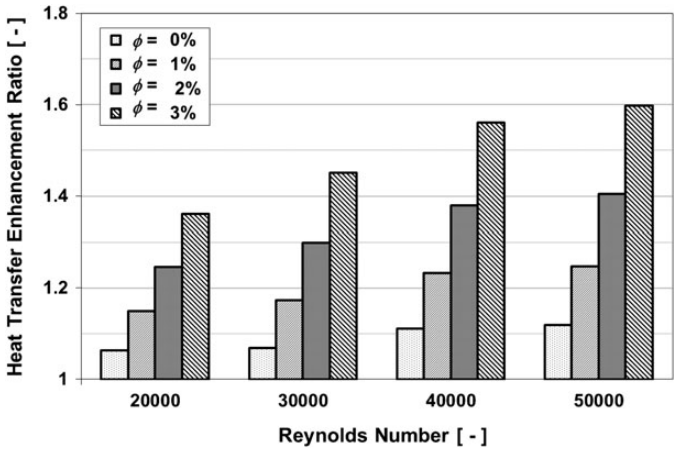

Figure 6. *Heat transfer enhancement ratio in helical coils.*

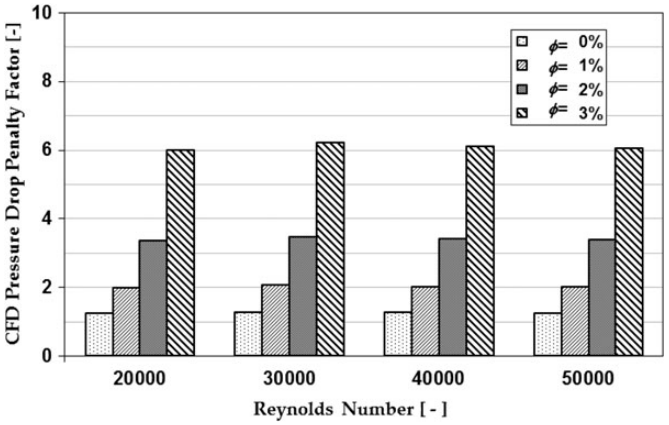

Figure 7. *Pressure drop penalty factor in helical coils.*

nanofluids at various Reynolds numbers. This figure shows that the heat transfer enhancement ratio increases with the nanofluid volume fractions due to enhanced nanofluid thermal transport properties and helical coil enhanced flow mixing. Also, increasing the Reynolds number further increases the heat transfer enhancement ratio. An enhancement ratio of up to 1.6 (60% enhancement) was achieved with 3% nanofluid volume concentration at Reynolds number of 50 000. At the same Reynolds number, the base fluid in the helical coil ($\phi = 0$), produced an enhancement ratio of 1.12. Thus, the addition of nanoparticles contributed with 80% of the 60% enhancement while the helical coiling contributed 20%.

Figure 7 shows the CFD results for the pressure drop ratio (nanofluid in helical coil to base fluid in straight tube) at various Reynolds numbers and volume concentrations. Results show that increasing the volume fraction increases the pressure drop ratio where a volume fraction of 3% produced six times the pressure drop of the base fluid in straight tube. This could be explained by the significant increase in the viscosity of the nanofluid for the same Reynolds number.

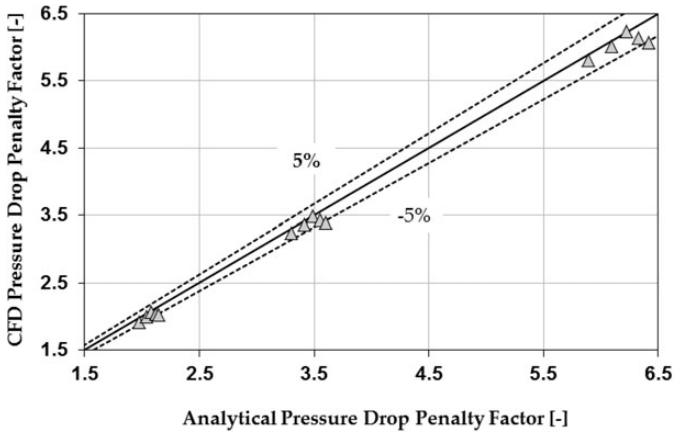

Figure 8. *Comparison of analytical pressure drop analysis and CFD prediction.*

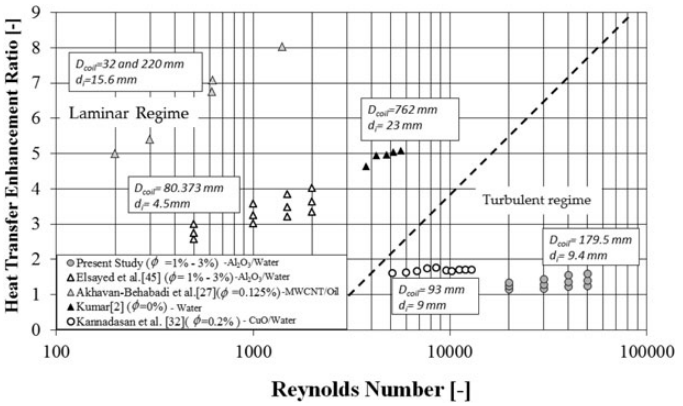

Figure 9. *Comparison of heat enhancement ratio in laminar and turbulent flow regimes.*

Using Darcy equation, the pressure ratio of nanofluids in helical coils compared with base fluid in straight tube can be expressed as:

$$\frac{\Delta p_{\mathrm{nf,Hc}}}{\Delta p_{\mathrm{bf,St}}} = \left(\frac{f_{\mathrm{nf,Hc}} L_{\mathrm{Hc}} + f_{\mathrm{nf,St}}(L_{\mathrm{tube}} - L_{\mathrm{Hc}})}{f_{\mathrm{bf,St}} L_{\mathrm{tube}}}\right)\left(\frac{\mu_{\mathrm{nf}}}{\mu_{\mathrm{bf}}}\right)^{2}\left(\frac{d_{\mathrm{nf}}}{d_{\mathrm{bf}}}\right)^{-3}\left(\frac{\rho_{\mathrm{nf}}}{\rho_{\mathrm{bf}}}\right)^{-1}, \quad (23)$$

where L_{tube}, L_{Hc} are the total straight tube lengths including the adiabatic parts and the coil length with 4319 and 2819 mm, respectively. The friction factor of nanofluid in helical coil $f_{\mathrm{nf,Hc}}$ was calculated using the White correlation [43] for turbulent flow. The friction factor of the nanofluid in the straight tube $f_{\mathrm{nf,St}}$ was taken as equal to that of the base fluid in a straight tube at the same Reynolds number, as recommended by Li and Xuan [10]. Thus:

$$\frac{f_{\mathrm{nf,Hc}}}{f_{\mathrm{bf,St}}} = \frac{f_{\mathrm{nf,Hc}}}{f_{\mathrm{nf,St}}} = \frac{4(0.08Re_{\mathrm{nf}}^{-0.25} + 0.012(d_i/d_{\mathrm{coil}})^{0.5})}{0.316Re_{\mathrm{nf}}^{-0.25}} \quad (24)$$
$$(15\,000 < Re < 100\,000),$$

where $f_{\mathrm{nf,Hc}}$ and $f_{\mathrm{nf,St}}$ are the friction factors of the nanofluids in helical coils and straight tubes based on White [43] and Blasius correlations [44] ($f_{\mathrm{Blasius}} = 0.316Re_{\mathrm{nf}}^{-0.25}$) using the nanofluid thermo-physical properties. Figure 8 compares the pressure drop ratio calculated using equations (23) and (24) with those predicted by the CFD with $\pm$5% relative deviation.

Figure 9 presents the heat transfer enhancement ratio (heat transfer coefficient of nanofluid in the helical coil divided by that of base fluid in the straight tube) versus Reynolds number for the present study compared with those of Kumar *et al.* [2], Fakoor-Pakdaman *et al.* [29], Kannadasan *et al.* [32] and Elsayed *et al.* [45] for both nanofluids and base fluids. It can be seen that nanofluid are more effective in enhancing the heat transfer in the laminar flow regime compared with the turbulent flow. In the laminar flow regime with thick boundary layers, the addition of nanoparticles increases the thermal conductivity and reduces the specific heat of the fluid resulting in a better dispersion of heat inside the fluid leading to steeper temperature gradient close to wall. As the flow becomes turbulent, the thermal boundary layer is already thin due to the nature of the flow. Therefore, the effect of adding nanoparticles on the thermal boundary layer is less significant.

5 CONCLUSIONS

The combined effect of using helical coils and nanofluids heat transfer enhancement and pressure losses in turbulent flow was numerically investigated. The developed CFD models were validated against published experimental data and empirical correlations. CFD results showed that using 3% volume fraction of Al_2O_3/water nanofluids in helical coils increased the heat transfer coefficient by up to 60% of that for pure water in straight tubes at the same Reynolds number. The contribution of tube coiling to this enhancement was shown to be only 10% on average.

Pressure drop values from CFD prediction and developed correlation were in close agreement, with less than $\pm$5% deviation. The pressure drop in helical coils using Al_2O_3 with volume fraction of 3% was six times that of water in straight tubes. With such modest improvement in heat transfer and high pressure losses, the adoption of such heat transfer enhancement techniques can only be justified in applications where improvements in heat transfer is very critical.

The long-term stability of nanofluids was reviewed by Ghadimi *et al.* [46]. They concluded that the stability of nanoparticles in the fluid depends mainly on the techniques used to prepare the nanofluid. Methods like ultrasonic, ph-control and using dispersants (Arabic Gum) have produced stable solutions.

REFERENCES

[1] Bergles AE. ExHFT for fourth generation heat transfer technology. *Exp Therm Fluid Sci* 2002;**26**:335–44.

[2] Kumar V, Saini S, Sharma M, *et al.* Pressure drop and heat transfer study in tube-in-tube helical heat exchanger. *Chem Eng Sci* 2006;**61**:4403–16.

[3] Wongwises S, Polsongkram M. Evaporation heat transfer and pressure drop of HFC-134a in a helically coiled concentric tube-in-tube heat exchanger. *Int J Heat Mass Transf* 2006;**49**:658–70.

[4] Elsayed A, Al-dadah R, Mahmoud S, *et al*. Experimental investigation of heat transfer in flow boiling inside a helically coiled small diameter tube. In *Proceedings of Microfluidics 2010 Conference, France*, MICROFLUIDICS2010/158, https://webistem.com/bin/pdfabstract?dir=microfluidics2010&ref=158.

[5] Wongwises S, Polsongkram M. Condensation heat transfer and pressure drop of HFC-134a in a helically coiled concentric tube-in-tube heat exchanger. *Int J Heat Mass Transf* 2006;**49**:4386–98.

[6] Shao L, Han Jt, Su Gp, *et al*. Condensation heat transfer of R-134A in horizontal straight and helically coiled tube-in-tube heat exchangers. *J Hydrodyn Ser B* 2007;**19**:677–82.

[7] Saripella SK, Routbort JL, Yu W, *et al*. Effects of nanofluid coolant in a class 8 truck engine. 2007. http://papers.sae.org/2007-01-2141 (5 April 2011, date last accessed).

[8] Cheng L. Nanofluid heat transfer technologies. *Recent Pat Eng* 2009;**3**:1–7.

[9] Sundar LS, Ramanathan S, Sharma KV, *et al*. Temperature dependent flow characteristics of Al_2O_3 Nanofluid. *Int J Nanotech Appl* 2007;**1**:35–44.

[10] Li Q, Xuan Y. Convective heat transfer and flow characteristics of Cu-water nanofluid. *Sci China Ser E* 2002;**45**:408–16.

[11] Nguyen CT, Roy G, Lajoie PR, *et al*. Nanofluids heat transfer performance for cooling of high heat output microprocessor. In *Proceedings of the 3rd IASME/WSEAS International Conference on Heat Transfer*. Corfu, Greece 2005, 160–5.

[12] Rostamani M, Hosseinizadeh SF, Gorji M, *et al*. Numerical study of turbulent forced convection flow of nanofluids in along horizontal duct considering variable properties. *Int Commun Heat Mass Transfer* 2010;**37**:1426–31.

[13] Torii S. Experimental study on convective heat transfer of aqueous suspension of nano-diamond particles. In *Proceedings of International Symposium on EcoTopia Science* 2007; 352–357.

[14] Bianco V, Manca O, Nardini S. Numerical investigation on nanofluids turbulent convection heat transfer inside a circular tube. *Int J Therm Sci* 2011;**50**:341–9.

[15] Pak B, Cho YI. Hydrodynamic and heat transfer study of dispersed fluids with submicron metallic oxide particle. *J Heat Transfer* 1998;**11**:151–70.

[16] Mangrulkar CK, Kriplani VM. Nanofluid heat transfer—a review. Int J Eng Tech *(IJET)* 2013;**3**:136–42.

[17] Sasmito AP, Kurnia JC, Mujumdar AS. Numerical evaluation of laminar heat transfer enhancement in nanofluid flow in coiled square tubes. *Nanoscale Res Lett* 2011;**6**:376.

[18] Akbarinia A, Behzadmehr A. Numerical study of laminar mixed convection of a nanofluid in horizontal curved tubes. *Appl Therm Eng* 2007;**27**:1327–37.

[19] Akbarinia A, Laur R. Investigating the diameter of solid particles effects on a laminar nanofluid flow in a curved tube using a two phase approach. *Int J Heat Fluid Flow* 2009;**30**:706–14.

[20] Huminic G, Huminic A. Heat transfer characteristics in double tube helical heat exchangers using nanofluids. *Int J Heat Mass Transf* 2011;**54**:4280–7.

[21] Mohammed HA, Narrein K. Thermal and hydraulic characteristics of nanofluid flow in a helically coiled tube heat exchanger. *Int Commun Heat Mass Transf* 2012;**39**:1375–83.

[22] Narrein K, Mohammed HA. Influence of nanofluids and rotation on helically coiled tube heat exchanger performance. *Thermochim Acta* 2013;**564**: 13–23.

[23] Akbaridoust F, Rakhsha M, Abbassi A, *et al*. Experimental and numerical investigation of nanofluid heat transfer in helically coiled tubes at constant wall temperature using dispersion model. *Int J Heat Mass Transf* 2013;**58**:480–91.

[24] Mukeshkumar PC, Kumar J, Suresh S, *et al*. Experimental study on parallel and counter flow configuration of a shell and helically coiled tube heat exchanger using Al2O3/water nanofluid. *J Mater Environ Sci* 2012;**3**:766–75.

[25] Kahani M, Zeinali Heris S, Mousavi SM. Comparative study between metal oxide nanopowders on thermal characteristics of nanofluid flow through helical coils. *Powder Tech* 2013;**246**:82–92.

[26] Hashemi SM, Akhavan-Behabadi MA. An empirical study on heat transfer and pressure drop characteristics of CuO–base oil nanofluid flow in a horizontal helically coiled tube under constant heat flux. *Int Commun Heat Mass Transf* 2012;**39**:144–51.

[27] Akhavan-Behabadi MA, Pakdaman MF, Ghazvini M. Experimental investigation on the convective heat transfer of nanofluid inside vertical helically coiled tubes under uniform wall temperature condition. *Int Commun Heat Mass Transf* 2012;**39**:556–64.

[28] Pakdaman MF, Akhavan-Behabadi MA, Razi P. An experimental investigation on thermo-physical properties and overall performance of MWCNT/heat transfer oil nanofluid flow inside vertical helically coiled tubes. *Exp Therm Fluid Sci* 2012;**40**:103–11.

[29] Fakoor-Pakdaman M, Akhavan-Behabadi MA, Razi P. An empirical study on the pressure drop characteristics of nanofluid flow inside helically coiled tubes. *Int J Therm Sci* 2013;**65**:206–13.

[30] Seban RA, Mclaughlin EF. Heat transfer in tube coils with laminar and turbulent flow. *Int Heat Mass Transf* 1963;**6**:387–95.

[31] Mori Y, Nakayama W. Study on forced convective heat transfer in curved pipes. *Int J Heat Mass Transf* 1967;**10**:681–95.

[32] Kannadasan N, Ramanathan K, Suresh S. Comparison of heat transfer and pressure drop in horizontal and vertical helically coiled heat exchanger with CuO/water based nano fluids. *Exp Therm Fluid Sci* 2012;**42**:64–70.

[33] Wallace KG. *Research in Heat Transfer with Nanofluids*. Master of Science in Technology, Purdue University Calumet School of Technology, 2010.

[34] Lotfi R, Saboohi Y, Rashidi AM. Numerical study of forced convective heat transfer of nanofluids: comparison of different approaches. *Int Commun Heat Mass Transf* 2010;**37**:74–8.

[35] Kalteh M, Abbassi A, Saffar-Avval M, *et al*. Eulerian–Eulerian two-phase numerical simulation of nanofluid laminar forced convection in a microchannel. *Int J Heat Fluid Flow* 2011;**32**:107–16.

[36] He Y, Men Y, Zhao Y, *et al*. Numerical investigation into the convective heat transfer of TiO_2 nanofluids flowing through a straight tube under the laminar flow conditions. *Appl Therm Eng* 2009;**29**:1965–72.

[37] Ansys Fluent user guide. Section 12.4.1.

[38] Williams W, Buongiorno J, Hu L. Experimental investigation of turbulent convective heat transfer and pressure loss of alumina/water and zirconia/water nanoparticle colloids (nanofluids) in horizontal tubes. *J Heat Transf* 2008;**130**:7.

[39] Kelecy FJ. Coupling momentum and continuity increases CFD robustness. *ANSYS Adv* 2008;**2**:49–51.

[40] Bejan A, Kraus A. *Heat Transfer Handbook*. John Wiley & Sons, Inc., 2003 (Chapter 11).

[41] Vajjha RS, Das DK, Kulkarni DP. Development of new correlations for convective heat transfer and friction factor in turbulent regime for nanofluids. *Int J Heat Mass Transf* 2010;**53**:4607–18.

[42] Maiga SEB, Nguyen CT, Galanis N, *et al*. Heat transfer enhancement in turbulent tube flow using Al2O3 nanoparticle suspension. *Int J Numer Methods Heat Fluid Flow* 2006;**16**:275–92.

[43] Welti-Chanes J, Vélez-Ruiz J, Barbosa-Cánovas JV. *Transport Phenomena in Food Processing*. CRC Press LLC, 2003 (Chapter 25).

[44] Kakaç S, Liu H. *Heat Exchangers: Selection, Rating and Thermal Design*, 2nd edn. CRC Press, 2002 (Chapter 4).

[45] Elsayed A, Al-dadah R, Mahmoud S, *et al*. Numerical investigation of laminar flow heat transfer through helically coiled tubes using Al_2O_3 nanofluid. In *3rd Micro and Nano Flows Conference.* , 2011.

[46] Ghadimi A, Saidur R, Metselaar HSC. A review of nanofluid stability properties and characterization in stationary conditions. *Int J Heat Mass Transf* 2011;**54**:4051–68.